

Preliminary probabilistic seismic hazard assessment for the Nuclear Power Plant Bohunice (Slovakia) site

P. Labák, A. Bystrická & P. Moczo

Geophysical Institute, Slovak Academy of Sciences, Dúbravská cesta 9, 842 28 Bratislava, Slovak Republic

K. W. Campbell

EQE International, Inc., 2942 Evergreen Parkway, Suite 302, Evergreen, CO 80439, USA

L. Rosenberg

Dept. of Geophysics, Fac. of Mat. & Physics, Comenius University, 842 15 Bratislava, Slovak Republic

Keywords: seismic hazard, probabilistic analysis

ABSTRACT: At the request of the Nuclear Power Plant (NPP) Bohunice we re-assessed the seismic design criteria for the Bohunice NPP site. Previous criteria were based on deterministic analyses. However the International Atomic Energy Agency (IAEA) has recommended that the new design criteria for the site should be based on a probabilistic seismic hazard analysis (PSHA). Based on this recommendation we have undertaken a comprehensive study of the geology, seismicity, seismic zoning and attenuation characteristics of the region within at least 150 km from the NPP site. The results of this study were used to develop uniform hazard spectrum (UHS) for the return period of 10,000 years and to define the response spectrum for the review level earthquake (RLE).

1 INTRODUCTION

Seismic hazard assessment and assessment of the seismic design criteria for critical facilities (e.g., nuclear power plants) is a very important task not only in the countries with strong and frequent earthquakes but also in the countries like Slovakia where only medium and sporadic earthquakes occur. Relatively rare occurrence of the earthquakes implies in general the problem of a lack of data for the seismic hazard assessment. This implies the necessity to use several alternative methods for assessing hazard. Both aspects lead to the generation of alternative input data sets for the seismic hazard assessment. The current methods developed in the countries with high seismic activity (e.g., EPRI 1986, Reiter 1990) for the probabilistic seismic hazard analysis enable to include various alternative data sets that enter computations. We tried to take the advantage of this also in the case of seismic hazard assessment for the Bohunice Nuclear Power Plant in Slovakia (BNPP).

2 SEISMOLOGICAL AND GEOLOGICAL DATABASES

2.1 *Seismological database*

We first compiled the seismological database. The database includes the data on macroseismically observed earthquakes (Figure 1) and instrumentally located earthquakes in the far region (region within at least 150 km far from the BNPP site), and data on instrumentally located microearthquakes in the near region (Figure 2) of the BNPP site (region within 35 km far from the site).

Data on historical earthquakes cover the largest part of the data on macroseismically observed earthquakes. Quality of data on the historic earthquakes depends mainly on the quality of primary, i.e.,

earthquake contemporary sources. Consistently processed primary sources are available in the studies of particular earthquakes that have been completed in the past 10 – 15 years. However, such studies are available only for some of the strongest earthquakes in the far region. The data on most of the earthquakes is taken from the descriptive and parametric catalogues. Descriptive catalogues (e.g., Réthly 1952, and Kárník et al. 1957) use either primary and secondary sources or secondary sources, i.e., sources from later time after the earthquake, only. The quality of sources has an impact on the uncertainty of earthquake parameters. The epicenter locations are given with an accuracy not better than ± 10 km (it is usually even as much as ± 20 km and more). Epicentral intensity is given with an accuracy not better than $\pm 0.5^\circ$ MSK-64 (the usual case is even up to $\pm 1^\circ$ MSK-64). Taking into account the number of earthquakes and the length of the period (more than 500 years) for which data on the historic earthquakes is available, this data on historic earthquakes represent the crucial part of the seismological database for the BNPP far region. However, the existing uncertainties of the epicenter locations and epicentral intensity estimation are relatively high.

Systematic seismometric observations have been available since WW II. However, the accuracy of the instrumental localization of earthquakes by the 60s is not better than that of the macroseismic localization. Reliable instrumental localizations are only available for a small number of the total of earthquakes in the BNPP far region. It is clear that the data on instrumentally localized earthquakes has only complementary character compared to the data on historic earthquakes.

Data on the microearthquake activity from the BNPP local network in the near region has been available since 1985. The localization accuracy for the epicenters of earthquakes with $M_1 \geq 1$ was usually ± 1 up to 2 km. Because of the character of the data on the historic earthquakes and instrumentally localized earthquakes, the seismometric data on microearthquakes from the local network of the BNPP is of the same relevance as that of the data on historic earthquakes for the determination of boundaries, and the way of simulating the closest source zone to the BNPP site – the Dobrá Voda source zone. More details about the seismological database are given in the report by Labák et al. (1997).

2.2 Geological database

The geological database consists of a description of the characteristics of basic geomorphologic and physiographic units, basic crustal blocks, structural development of sedimentary basins, Quaternary deformation, and geophysical parameters (Bouguer anomalies, magnetic anomalies, thickness of the lithosphere and MOHO, heat flow density, recent vertical movements, data on boreholes and results of deep seismic sounding) for the far region, and geomorphologic classification, geologic structure, structural analysis and geophysical characteristics (including data from gravimetric, geomagnetic, geoelectric, seismic reflection and logging surveys) for the near region. More details about the database are given in the report by EQUIS (1997).

3 SEISMOTECTONIC MODEL

3.1 Source zones

Taking into account the large uncertainty in the location of macroseismically observed earthquakes we used only areal sources to define the seismicity in the far region. Uncertainty in the

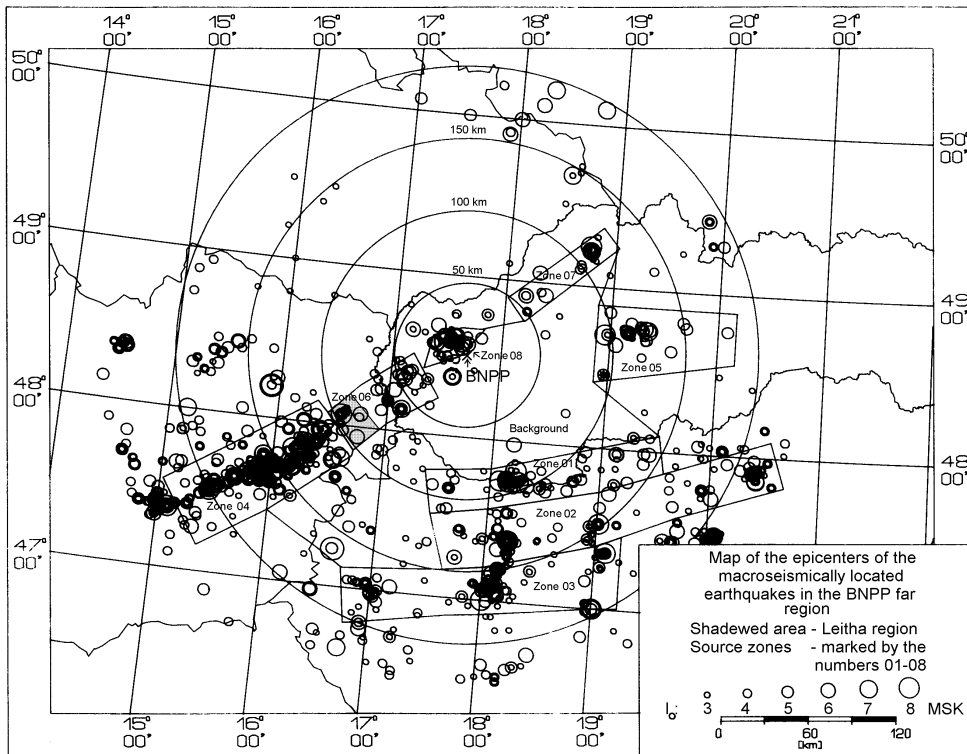


Figure 1. Map of the epicenters of the macroseismically observed earthquakes in the far region of the BNPP. Shaded area corresponds to the Leitha region. Source zones are marked by numbers 01-08.

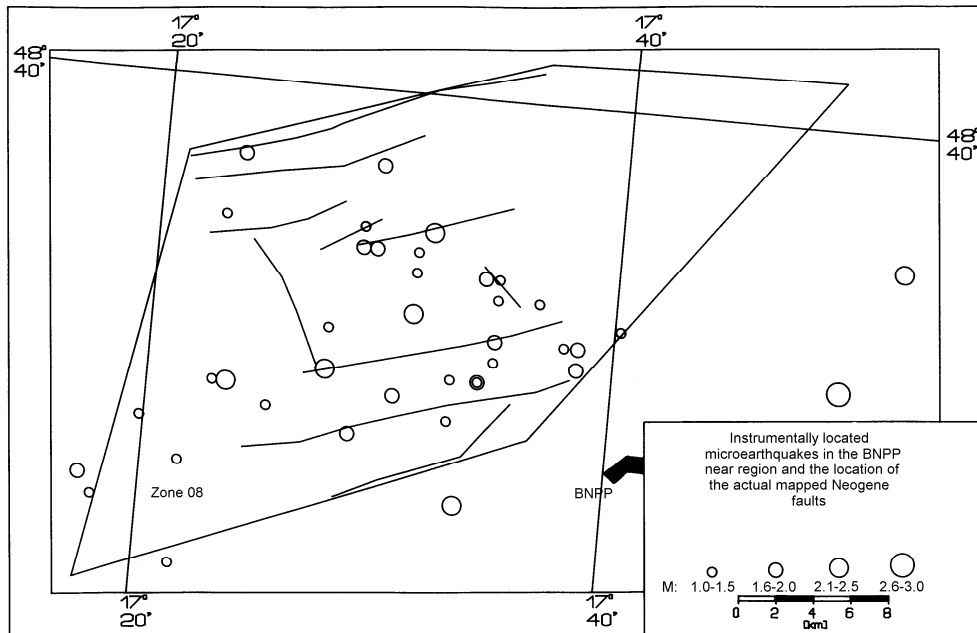


Figure 2. Map of the epicenters of the instrumentally located microearthquakes and actual mapped Neogene faults in the Dobrá Voda source zone (Zone 08).

databases led us to define two alternative source zonation models for the Eastern Alps – Western Carpathians junction area in the far region. Figure 1 shows both source zonation models. The Leitha region (shaded area) belongs to the Western Carpathians (to the zone 06) in the first alternative of the zonation. This interpretation is based on geological data (not shown here). In the other alternative of the source zonation the Leitha region belongs to the Eastern Alps (to the zone 04). This alternative is supported by clustering of the epicenters of macroseismically observed earthquakes (shown in the figure).

The higher resolution of the geological and seismological data in the near region allowed us to model the closest earthquake source zone to the BNPP site, the Dobrá Voda zone (zone 08 in Figure 1), as a system of faults. We used three modeling alternatives for this zone. One alternative was based on the actual location of the mapped Neogene faults (Figure 2). The other two alternatives were based on two different descriptions of distributed faults. The distributed faults have the prevailing orientation of the real faults in both alternatives. In the first alternative the distributed faults are 3 km apart and in the second alternative 6 km apart. Both these distances are typical in distribution of the real faults (see Figure 2).

Combining the alternative source zonation models – two in the far region and three in the near region, we obtained six possible zonation models.

The area between the defined source zones is covered by the Background source zone in all the alternatives.

3.2 *Minimum magnitude*

For the minimum magnitude we chose the surface-wave magnitude value $M_s = 4.33$ which corresponds with the moment magnitude $M = 5$ (see Chapter 4 for the conversion between the values of the moment magnitude and magnitude M_s). The study of EPRI (1993) shows that such a value of the minimum magnitude is suitable for nuclear power plants and other similar building structures because in the case of occurrence of such an earthquake or a weaker one in the immediate surrounding of a nuclear power plant site, the nuclear power plant should not be damaged. Taking into account the current situation of upgrading power plant, the choice of the minimum magnitude $M = 5$ is adequate also for the BNPP site.

3.3 *Maximum magnitude*

Because of a small number of data we defined the maximum magnitude jointly for the group of the source zones which belong to the same basic geologic-tectonic unit, i.e. jointly for the source zones in the Western Carpathians (zones 05-08), for the zone in the Eastern Alps (zone 04), and jointly for the zones in the Pannonian region (zones 01-03).

We used four alternatives for defining the maximum magnitude. The first two alternatives were to add 0.5 and 1.0 to the observed maximum magnitude. We used the magnitudes which were assessed from the values of epicentral intensities. This magnitudes correspond to the surface-wave magnitudes (Kárník 1968).

In the third alternative the maximum magnitude values were computed from the Gumbel Type III asymptotic distribution of extreme values (Gumbel 1959, Yegulalp & Kuo 1974).

Unlike the first three alternatives, the fourth one was used only for the Dobrá Voda source zone. The maximum magnitude was computed from the relationship between fault rupture lengths and earthquake magnitude developed from worldwide data (Wells & Coppersmith 1994). This was possible due to the modeling of the Dobrá Voda source zone as a system of faults. We used the following two formulae for all slip types:

$$M = 5.08 + 1.16 * \log (\text{SRL}) \quad (1)$$

where M is the moment magnitude and SRL is the surface rupture length, and

$$M = 4.38 + 1.49 * \log (\text{RLD}) \quad (2)$$

where RLD is the subsurface rupture length. We identified the SRL with the maximum surface length of the real faults (about 20 km) and the RLD with the maximum length of distributed faults (about 35 km). We also transformed the moment magnitude values into the surface-wave magnitude values.

Except for the fourth approach we used all the other approaches also for the definition of the maximum magnitude for the Background. Because of the specific character of the zone, we defined the maximum magnitude as the mean value of all values computed for this zone in all the alternatives.

Table 1 shows the final maximum magnitude values M_S in the individual alternatives of the maximum magnitude definition.

3.4 Magnitude-frequency relationships

We computed the cumulative magnitude-frequency relationships for each source zone using the maximum-likelihood method (Weichert 1980) for the surface-wave magnitude values. We selected the earthquakes for each zone in two different ways. Either we only used the earthquakes which had epicenters within the defined source zone (Figure 1) or, in order to take into account the error in location of the macroseismically observed earthquakes, we alternatively included those earthquakes from a larger region around each of the zones (Figure 3). Gutenberg-Richter b-values were

Table 1. Maximum magnitude values M_S for the four alternatives of the maximum magnitude determination.

Source zones	1 st alternative	2 nd alternative	3 rd alternative	4 th alternative
in the Western Carpathians (except for Dobrá Voda)	6.3	6.8	6.2	as in the 3 rd alternative
in the Dobrá Voda source zone	as in the Western Carpathians	as in the Western Carpathians	as in the Western Carpathians	6.5/6.6*
in the Eastern Alps	5.9	6.4	5.8	as in the 3 rd alternative
in the Pannonian region	6.3	6.8	7.1	as in the 3 rd alternative
in the Background source zone	5.5	5.5	5.5	as in the 3 rd alternative

* The first value corresponds to the model of real faults, the other value to the models of distributed faults

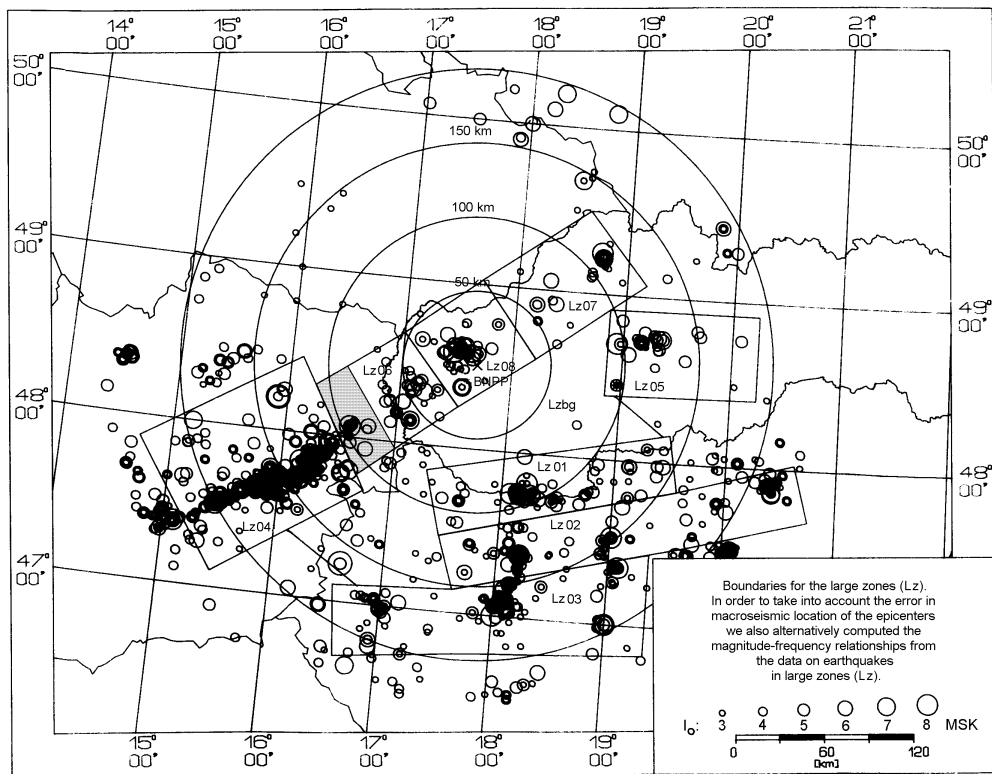


Figure 3. Boundaries of the large zones (Lz). In order to take into account the error in the macroseismic location of the epicenters we also alternatively computed the magnitude-frequency relationships from the data on earthquakes in the large zones (Lz). (Compare with Figure 1). Shaded area corresponds to the Leitha region.

alternatively computed from either the data of individual source zones, or from the combined data of source zones belonging to the same basic geologic-tectonic unit (Western Carpathians, Eastern Alps, and Pannonian region). Uncertainty in the magnitude-frequency relationships was included by using three estimates of the activity rate: the mean and the plus and minus one standard error. In this way we obtained 12 different magnitude-frequency relationships for each source zone.

4 ATTENUATION

Since there are no strong motion records in the region, macroseismic intensity attenuation relationships were developed instead for the Western Carpathians (Bystrická et al. 1997), where the BNPP site is located. These intensity attenuation relationships were also compared with those for other regions for which strong motion records are available. It was found that the intensity attenuation in the Western Carpathians is similar to the intensity attenuation in California and the Balkan region. Based on this comparison, we selected peak ground acceleration (PGA) and spectral acceleration attenuation relationships developed for these analogous regions. We selected five different attenuation relationships. Four of them (Abrahamson & Silva 1997, Boore et al. 1997, Campbell 1997, and Sadigh et al. 1997) are from the Western United States. We used the fifth one, developed for all of Europe (Ambraseys et al. 1996), because of its similarity to attenuation relationships for the Western United States.

We derived the magnitude-frequency relationships for the M_S values. Except of Ambraseys et al. (1996) all the other attenuation relationships need the moment magnitude values. Therefore we had to convert the M_S values in to the moment magnitude M values. We used the Ekström & Dziewonski (1988) relationship between the seismic moment M_0 and the surface-wave magnitude M_S

$$\log M_0 = \begin{cases} 19.24 + M_S & M_S < 6.8 \\ 30.20 - \sqrt{(92.45 - 11.40 * M_S)} & 5.3 \leq M_S \leq 6.8 \\ 16.14 + 1.5 * M_S & M_S > 6.8 \end{cases} \quad (3)$$

and the Hanks & Kanamori (1979) relationship between the moment magnitude M and the seismic moment M_0

$$M = (2/3) * \log M_0 - 10.7. \quad (4)$$

These relationships were derived from the data of earthquakes all over the world. In the work of Ambraseys & Free (1997) an empirical relationship between M_0 and M_S for the region of Europe is derived. However, this relationship differs from (3) only a little.

We used the SEISRISK III program for the probabilistic seismic hazard computation (see Chapter 5). The program requires applying the r_{jb} distance. However, the attenuation relationships chosen by us use different types of the distances – the ‘Joyner-Boore distance’ r_{jb} , which is the closest horizontal distance to the vertical projection of the rupture, r_{rup} – the closest distance to the rupture surface, and r_{seis} – the closest distance to the seismogenic rupture surface. In order to convert the r_{rup} and r_{seis} distances into the r_{jb} distance we used the following formula published by Campbell (1997) first:

$$d_{seis} = (1/2) * (H_{BOT} + H_{TOP} - W * \sin(\alpha)) + H_{TOP}. \quad (5)$$

Here d_{seis} is the average depth to the top of the seismogenic rupture zone; H_{TOP} and H_{BOT} are the depths to the top and bottom of the seismogenic part of the crust; α is a dip angle of the fault plane (in our case it is equal to 90° because the SEISRISK III program assumes that the faults included in the computation are perpendicular to the free surface), and W is the expected width (down-dip dimension) of the fault rupture in km calculated by applying the Wells & Coppersmith (1994) formula

$$\log W = -1.01 + 0.32 * M \quad (6)$$

where M is the moment magnitude. Taking into consideration the distribution of depths of epicenters in the BNPP far region, we put H_{BOT} equal to 15 km. The relationships between r_{rup} and r_{jb} and between the r_{seis} and r_{jb} are then expressed by the formulae

$$r_{rup} = \sqrt{(r_{jb}^2 + d_{seis}^2)} \text{ and } H_{TOP} = 0 \text{ km}, \quad r_{seis} = \sqrt{(r_{jb}^2 + d_{seis}^2)} \text{ and } H_{TOP} = 3 \text{ km}. \quad (7)$$

We determined H_{TOP} in (7) on the basis of the distribution of depths of epicenters in the BNPP region.

We set the optional parameters in the attenuation relationships so that way that they fit best the real conditions at the BNPP site and in the whole far region.

5 PROBABILISTIC COMPUTATIONS AND RESULTS

In order to include all alternative sets of input parameters in the hazard computation we constructed a logic tree. We defined 6 branches for the earthquake source zonation, 4 branches for the maximum magnitude, 12 branches for the magnitude-frequency relationships and 5 branches for attenuation. The whole logic tree has 1440 scenarios (Figure 4). The probability of each branch was assessed by expert judgment. We performed the seismic hazard computation for each scenario of the logic tree using the computer program SEISRISK III (Bender & Perkins 1987). We also simulated the logic tree using 100,000 Monte Carlo simulations.

The results were displayed as a series of seismic hazard curves representing the mean, 16%, 50% (median) and 84% confidence levels. Figure 5 shows an example of the hazard curves for the PGA obtained in the logic tree computation.

We found the results given by Monte Carlo simulations to be within 5% of those based on the 1440 logic tree scenarios for the mean and 84% and for the 10,000-year return period.

The hazard curves were used to estimate the values of PGA and spectral acceleration at the natural periods ranging from 0.1s to 2s for return periods of 10,000 years and all confidence levels. We defined the uniform hazard spectrum (UHS) as the mean response spectrum for the 10,000-year return period.

We used the mean 0.2 s UHS value for the de-aggregation of the logic tree computation and computation of the magnitude and distance of the controlling earthquake. We used similar approach as described in the report by Bernreuter et al. (draft).

In the step 1 we divided the whole BNPP far region into distance bins of 0-5 km, 5-10 km, 10-20 km, 20-40 km, 40-80 km and more than 80 km from the BNPP site.

In the step 2 we divided the whole magnitude interval starting from the minimum magnitude value (see section 3.2) up to the biggest value of the maximum magnitude (see Table 1) into the magnitude bins of the identical size, namely 4.33-4.82, 4.83-5.32, 5.33-5.82, 5.83-6.32, 6.33-6.82, and more than 6.82.

In the step 3 we performed the complete logic tree computations for all magnitude-distance bins.

In the step 4 we determined fractional relative contributions to the total probability of exceeding for the original 0.2 s UHS value (Figure 6) according to the formula

$$P_{M D} = \frac{H_{M D}}{\sum_m \sum_d H_{m d}} \quad (8)$$

where $P_{M D}$ is the fractional relative contribution of the magnitude-distance bin $M D$; $H_{M D}$ is the computed probability of exceeding in the step 3 for the magnitude-distance bin $M D$; and the $\sum_m \sum_d H_{m d}$ is the sum of probabilities of exceeding for all magnitude-distance bins.

In the step 5 we computed the magnitude M_C and distance D_C of the controlling earthquake according to the formulae

$$M_C = \sum_m M_m \sum_d P_{m d} \quad \text{and} \quad \ln(D_C) = \sum_d \ln(D_d) \sum_m P_{m d} \quad (9)$$

where M_m is the mean value of the magnitude bin m , D_d is the centroid value of the distance bin d and $P_{m d}$ is the fractional relative contribution to the magnitude-distance bin $(m d)$ to the total

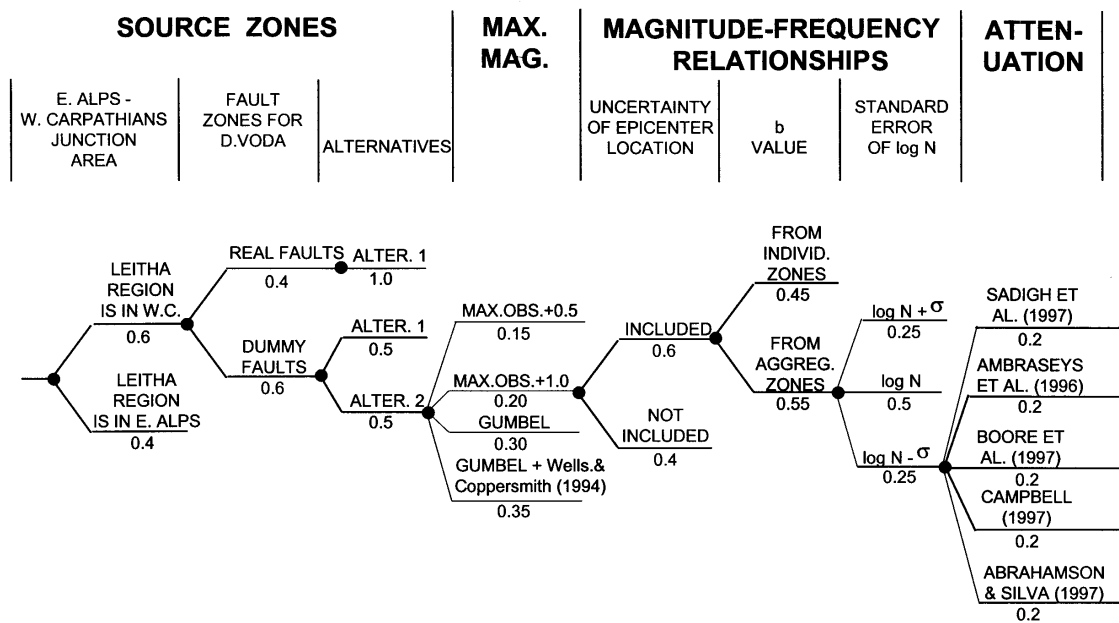


Figure 4. Simplified logic tree for the probabilistic seismic hazards computation for the BNPP site. Black circles correspond to nodes of the logic tree and lines correspond to branches. The probability of each branch is shown below the branch lines.

probability of exceeding (see formula 8). The surface-wave magnitude of the controlling earthquake is 5.86 and the r_{jb} distance of the controlling earthquake is 12.2 km. These values are similar to the values of the magnitude ($M=6$) and distance (epicentral distance 10 km and focal depth 10-20 km) of the so-called big earthquake in the previous deterministic study by Shteinberg et al. (1988).

Using the same five attenuation relationships from the probabilistic computations (see Chapter 4) we computed a mean spectrum for the values of magnitude and distance of the controlling earthquake. Scaling the mean spectrum to the 0.2 s UHS value we obtained the response spectrum for the Review Level Earthquake (RLE). Figure 7 shows the computed RLE response spectrum, response spectrum of the interim RLE from the report by EQE (1996) and the three response spectra – the mean response spectrum of artificial accelerograms, spectrum computed from some selected accelerograms, and the standard spectrum – from the report by Shteinberg et al. (1988). The interim RLE spectrum by EQE (1996) is within 15% of the RLE spectrum. The RLE spectrum is lower at almost all periods in comparison with the Shteinberg et al. (1988) spectra.

6 CONCLUSION

Despite the typical situation in the countries with the medium seismic activity we tried to assess the seismic hazard and seismic design criteria using the approach which is mainly used in the countries with higher seismic activity. In addition to the relationships between different characteristics developed from the local data which we needed (e.g., the relationships between epicentral intensity and magnitude, relationships for the macroseismic depth estimation), we had to use also the relationships estimated for other regions or from the worldwide data. In these cases we used only those relationships which were estimated either for regions analogous to the Western Carpathians (for example the PGA and spectral acceleration attenuation relationships in Chapter 4) or which were estimated from the data

of the same kind of the region as the Western Carpathians are, i.e. from the active regions with shallow crustal earthquakes. The logic tree approach allowed us to include several alternative input data sets in the seismic hazard computation.

The results show that while our probabilistic PGA value for the RLE and the values of magnitude and distance of the controlling earthquake are very similar to those estimated in the previous deterministic study by Shteinberg et al. (1988), the whole response spectrum for the RLE differs from the response spectra estimated in the report by Shteinberg et al. (1988). We also showed that the RLE response spectrum is within 15% of the interim RLE spectrum from the report by EQE (1996).

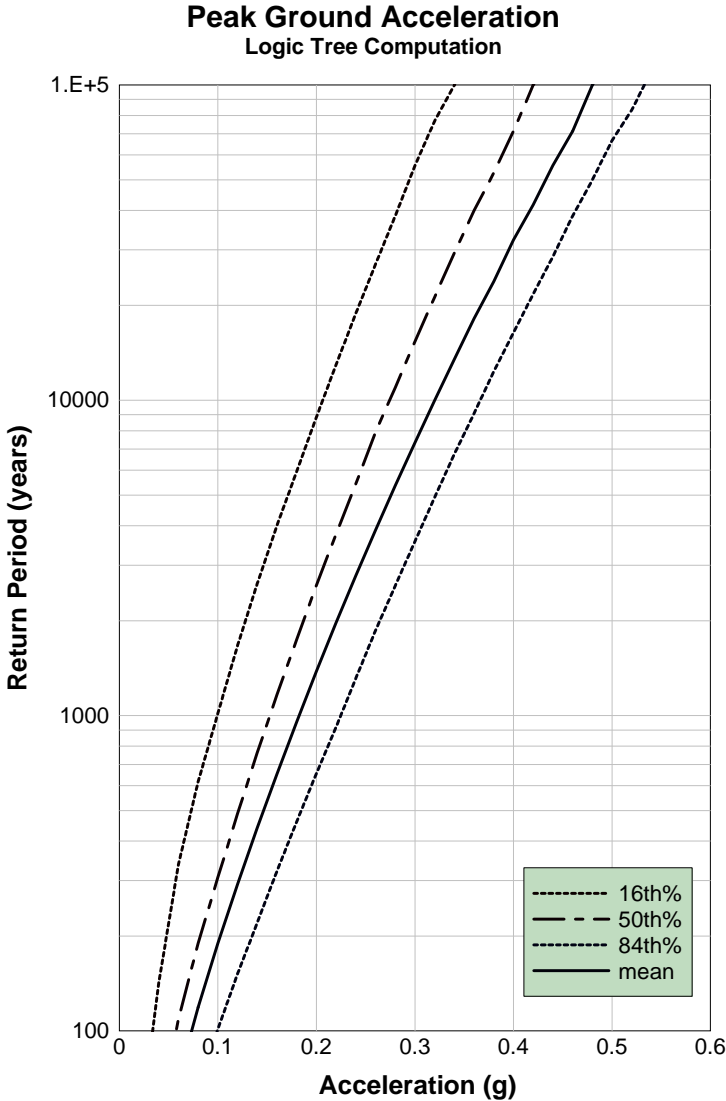


Figure 5. PGA hazard curves for the 16%, 50%, 84%, and mean confidence levels from the logic tree computation.

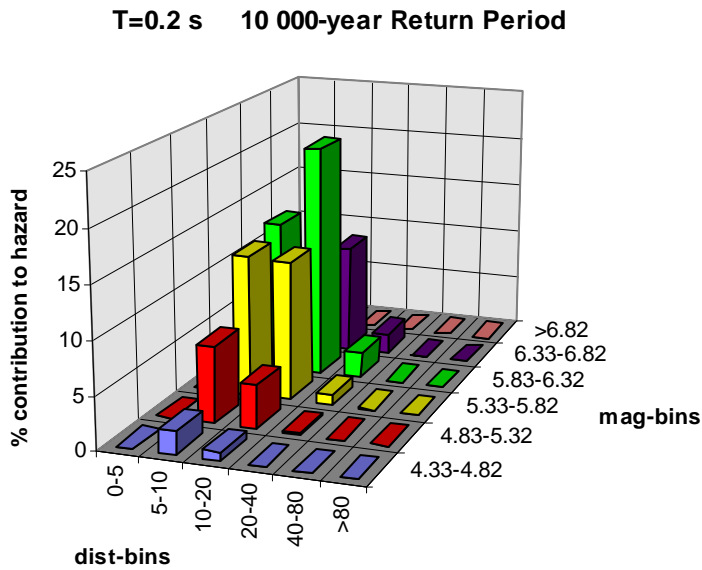


Figure 6. Fractional relative contribution in % to the total probability of exceeding for particular magnitude-frequency bins. The contributions were computed for the mean 0.2s 10,000-year ground motion value.

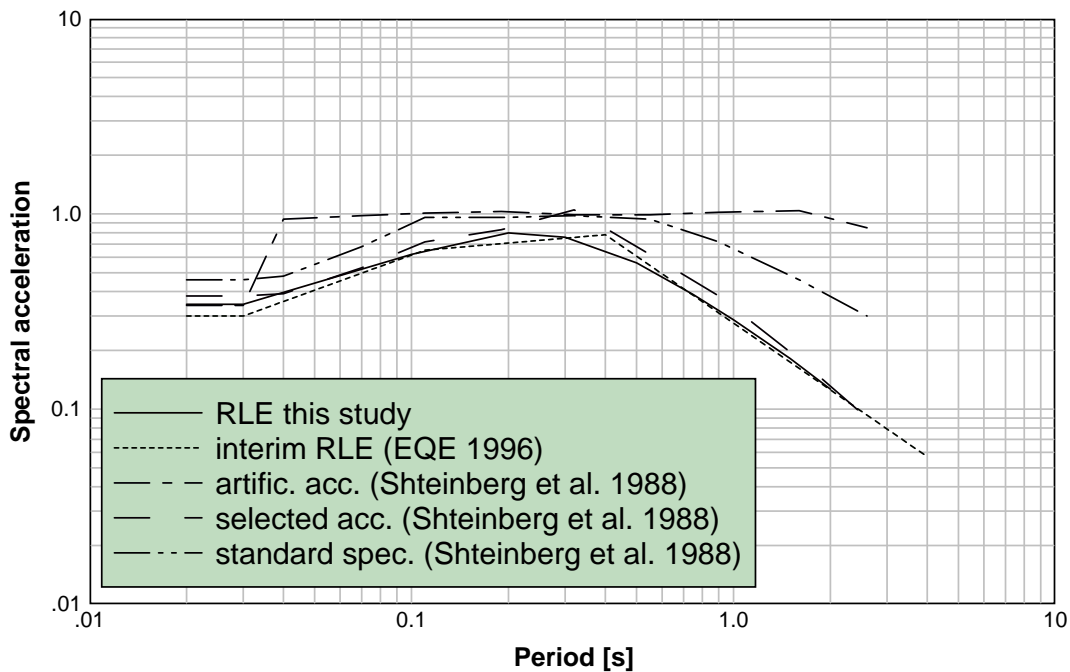


Figure 7. Computed RLE response spectrum, response spectrum of the interim RLE from the EQE (1996) report and the three response spectra – the mean response spectrum of artificial accelerograms, spectrum computed from some selected accelerograms, and the standard spectrum – from the report by Shteinberg et al. (1988).

REFERENCES

- Abrahamson, N. A., Silva, W. J., 1997. Empirical response spectral attenuation relations for shallow crustal earthquakes. *Seismological Research Letters*, 68, 94-127.
- Ambraseys, N. N., Free, M. W., 1997. Surface-wave magnitude calibration for European region earthquakes. *Journal of Earthquake Engineering*, 1, 1-22.
- Ambraseys, N. N., Simpson, K. A., Bommer, J. J., 1996. Prediction of horizontal response spectra in Europe. *Earthquake Engineering and Structural Dynamics*, 25, 371-400.
- Bender, B., Perkins, D. M., 1987. Seisrisk III: a computer program for seismic hazard estimation. *U. S. Geological Survey Bulletin 1772*. 48p.
- Bernreuter, D. L., Boissonnade, A. C., Short, C. M., draft. *Investigation of techniques for the development of seismic design basis using the probabilistic seismic hazard analysis*. Lawrence Livermore National Laboratory. Prepared for U.S. Nuclear Regulatory Commission, Office of Nuclear Regulatory Research, Washington.
- Boore, D. M., Joyner, W. B., Fumal, T. E., 1997. Equations for estimating horizontal response spectra and peak acceleration from Western North American earthquakes: A summary of recent work. *Seismological Research Letters*, 68, 128-153.
- Bystrická, A., Labák, P., Campbell, K. W., 1997. Intensity attenuation relationships for Western Carpathians and their comparison with other regional relationships. In: *Proc. of the 29th General Assembly of the IASPEI, Aug. 18-28, 1997, Thessaloniki, Greece*, p. 40. (abstract)
- Campbell, K. W., 1997. Empirical near-source attenuation relationships for horizontal and vertical components of peak ground acceleration, peak ground velocity, and pseudo-absolute acceleration response spectra. *Seismological Research Letters*, 68, 154-179.
- Ekström, G., Dziewonski, A. M., 1988. Evidence of bias in estimations of earthquake size. *Nature*, 332, 319-323.
- EPRI, 1986. *Seismic Hazard Methodology for the Central and Eastern United States*. EPRI NP-4726.
- EPRI, 1993. Method and guidelines for estimating earthquake ground motion in Eastern North America. In: *Guidelines for determining design basis ground motions, Vol. 1*, Electric Power Research Institute, Palo Alto, California, Report No. EPRI TR-102293.
- EQE, 1996. *Preliminary probabilistic seismic hazard assessment and interim review level earthquake for the Bohunice nuclear power plant, Republic of Slovakia*. EQE International.
- EQUIS, 1996. *Geological assessment of the Bohunice NPP region*. EQUIS, Bratislava. (in Slovak)
- Gumbel, E. J., 1959. *Statistics of extremes*. Columbia University Press, New York.
- Hanks, T. C., Kanamori, H., 1979. A moment magnitude scale. *Journal of Geophysical Research*, 84, B5, 2348-2350.
- Kárník, V., 1968. *Seismicity of the European area. Part 1*. Academia, Praha.
- Kárník, V., Michal, E., Molnár, A., 1957. Erdbebenkatalog der Tschechoslowakei bis zum Jahre 1956. *Travaux Géophysiques*, No. 69, Praha.
- Labák, P., Moczo, P., Bystrická, A., 1997. *Seismological database for the complex evaluation of the seismic hazard of the Bohunice NPP site*. Geophysical Institute, Slovak Academy of Sciences, Bratislava.
- Reiter, L., 1990. *Earthquake hazard analysis. Issues and insights*. Columbia University Press. New York.
- Réthly, A., 1952. *Earthquakes in the Carpathian basins 455-1918*. Akadémiai Kiadó, Budapest. (in Hungarian)
- Sadigh, K., Chang, C.-Y., Egan, J. A., Makdisi, F., Youngs, R. R., 1997. Attenuation relationships for shallow crustal earthquakes based on Californian data. *Seismological Research Letters*, 68, 180-189.
- Shteinberg, V. V., Krestnikov, V. N., Bune, B. I., Šimůnek, P., Barták, V., 1988. *Conclusions on the seismic safety of the Bohunice nuclear power plant*. Institute of the Physics of the Earth, Academy of Sciences of the USSR, Moscow, Energoprojekt, Praha. (in Russian)
- Weichert, D. H., 1980. Estimation of the earthquake recurrence parameters for unequal observation periods for different magnitudes. *Bulletin of the Seismological Society of America*, 70, 1337-1346.
- Wells, D. L., Coppersmith, K. J., 1994. New empirical relationships among magnitude, rupture length, rupture width, rupture area, and surface displacement. *Bulletin of the Seismological Society of America*, 84, 974-1002.
- Yegulalp, T. M., Kuo, J. T., 1974. Statistical prediction of the occurrence of maximum magnitude earthquakes. *Bulletin of the Seismological Society of America*, 64, 393-414.